

Synergistic Modulation Of Apoptotic Proteins By Curcumin And Chemotherapeutics: An Integrative Docking, Molecular Dynamics, And Free Energy Study

R. Mohan¹, S. Suja^{2*}, Abirami. S³, Sindhu. B⁴, Sneha. S⁵, Kanimozhi. A⁶, M. Subasri⁷

¹Department of Biochemistry, Bharathiar University, Coimbatore, India – 631046

²Department of Biochemistry, Bharathiar University, Coimbatore, India – 631046

³Pasteur Institute of India, Coonoor, India - 643103

⁴Pasteur Institute of India, Coonoor, India - 643103

⁵Pasteur Institute of India, Coonoor, India - 643103

⁶Department of Biochemistry, Bharathiar University, Coimbatore, India – 631046

⁷Department of Biochemistry, Bharathiar University, Coimbatore, India – 631046

*Corresponding author

S. Suja

ABSTRACT

Background: Apoptosis is central to breast cancer (BC) regulation, and its disruption promotes tumor progression and therapy resistance. Restoring apoptotic balance can enhance treatment outcomes.

Objective: To evaluate the anticancer potential of Curcumin (CUC), Docetaxel (DOC), and Carboplatin (CAP) against key apoptotic proteins in BC using integrative computational approaches.

Subjects and Methods: Apoptotic regulators including BAX, Caspase-9, Caspase-8, Caspase-3, BCL2, Wnt, and Integrin were analyzed using molecular docking, 200 ns molecular dynamics (MD) simulations, and MM-PBSA calculations to assess binding affinity, stability, and energetic contributions of single and combination drug interactions.

Results: CUC showed strong affinity for BAX and Caspase-9, while the CUC-DOC-CAP triple complex exhibited the greatest stability and lowest binding free energy among all systems. MD simulations confirmed enhanced compactness, sustained hydrogen bonding, and synergistic interactions, with MM-PBSA analysis indicating cooperative van der Waals and electrostatic contributions driving the superior stability of the triple-ligand complex.

Conclusion: CUC enhanced the chemotherapeutic performance of DOC and CAR by strengthening pro-apoptotic protein interactions, suggesting its promise as a chemosensitizer in BC therapy.

KEYWORDS: Breast cancer, apoptosis, curcumin, docetaxel, carboplatin, molecular docking, molecular dynamics, MM-PBSA

How to Cite: R. Mohan, S. Suja, Abirami. S, Sindhu. B, Sneha. S, Kanimozhi. A6, M. Subasri, (2025) Synergistic Modulation Of Apoptotic Proteins By Curcumin And Chemotherapeutics: An Integrative Docking, Molecular Dynamics, And Free Energy Study, Vascular and Endovascular Review, Vol.8, No.5s, 437-447.

INTRODUCTION

Breast cancer is the most common malignancy among women and the second leading cause of cancer-related deaths worldwide, accounting for nearly one-fourth of all female cancers [1, 2]. Over 1.5 million new cases are reported each year [3, 2] with India contributing about 28.2% of all female cancers [4]. Despite advancements in surgery, radiotherapy, chemotherapy, and targeted therapies, challenges such as toxicity, multidrug resistance, and high metastatic potential persist [5, 6, 7, 8].

Combination therapy offers a promising strategy to enhance efficacy, modulate multiple signaling pathways, and mitigate resistance through synergistic effects [9,10]. Curcumin (CUC), a polyphenolic compound from Curcuma longa, exhibits anti-proliferative, pro-apoptotic, and anti-metastatic activities across various cancers [11, 12, 13]. Its combination with carboplatin (CAP) or docetaxel (DOC) improves therapeutic outcomes and reduces systemic toxicity [14,15, 16].

In this study, we developed a triple-drug combination of curcumin, carboplatin, and docetaxel (CUC-CAP-DOC) for targeted Breast Cancer therapy. While dual combinations like CUC-CAP and CUC-DOC have been explored, the CUC-CAP-DOC formulation is novel. Using molecular docking and molecular dynamics simulations, we analyzed ligand-protein interactions, stability, and binding energetics to elucidate its synergistic anticancer potential and therapeutic mechanism in breast cancer.

NEED FOR THE STUDY

Binary combinations of CUC with conventional drugs have shown significant promise, but their mechanisms and efficacy remain limited. A novel triple formulation CUC-CAP-DOC could provide enhanced selectivity, improved drug delivery, and stronger synergistic effects against BC. To uncover the molecular mechanisms involved, computational methods such as molecular docking and molecular dynamics simulations were employed. This study aims to evaluate the structural and energetic basis of

the CUC-CAP-DOC combination to support its development as a safer and more effective therapeutic option for breast cancer.

MATERIALS AND METHODS:

Molecular Docking

The crystal structures of target proteins BAX, Caspase-9, Caspase-8, Caspase-3, BCL2, Wnt, and Integrin were retrieved from the Protein Data Bank [17, 18, 19]. Using Discovery Studio 4.5, receptor structures were preprocessed by removing water molecules, ions, and preexisting ligands, while ligands were energy-minimized and converted to mol2 format. Open Babel was used to generate pdbqt files [20]. Hydrogen atoms were added to receptor molecules using AutoDock Vina, and grid maps were constructed with AutoGrid (grid size 90 Å \times 90 Å) under default settings [21, 22]. The 2D ligand–receptor interactions were further analyzed using Discovery Studio 4.5 [23, 24].

Table 1 Structural details and active site coordinates of selected protein target

S. No	Protein targets	PDB ID	Resolution Å	Active site coordinates		
				X	Y	Z
1	BAX	5W60	1.80 Å	-22.163	-1.116	5.627
2	Caspase-9	1JXQ	2.80 Å	21.716	34.074	-17.317
3	Caspase-8	3KJN	1.80 Å	-11.529	32.574	42.147
4	Caspase-3	3DEI	2.80 Å	-52.086	16.514	-21.668
5	BCL2	600K	1.62 Å	-9.986	2.205	-18.501
6	Wnt	7URD	2.92 Å	113.368	112.001	112.029
7	Integrin	1L5G	3.20 Å	-12.69	19.62	49.5799

Molecular dynamics (MD) simulation:

Molecular dynamics (MD) simulations were performed using GROMACS 2019 to validate docking results and assess protein—ligand stability over 200 ns [25, 26]. Complexes included BAX (BAX-APO, BAX-CUC, BAX-CUC-DOC, BAX-CUC-DOC-CAP) and Caspase-9 (CAS-APO, CAS-CUC, CAS-CUC-DOC, CAS-CUC-DOC-CAP). Ligand topologies were generated using Antechamber, and hydrogens were added via pdb2gmx. Systems were mimized using the steepest descent method (1500 steps), solvated with the SPCE water model, and neutralized with Na⁺ and Cl[−] ions at 0.15 M concentration. Equilibrated systems underwent 200 ns production runs under the NPT ensemble [27, 28, 29]. Analyses included RMSD, RMSF, Rg, SASA, and secondary structure evaluations using "gmx rmsd," "gmx rmsf," "gmx gyrate," "gmx sasa," and "gmx do_dssp" tools. Stable trajectories (≥60 ns) were analyzed within 5 ns windows, and structural visualization was performed using VMD and PyMol [30].

Free-Energy Calculations

Binding free energy (Δ Gbinding) of protein–ligand complexes was evaluated using the Molecular Mechanics Poisson–Boltzmann Surface Area (MM-PBSA) method with the GROMACS utility g_mmpbsa [31, 32]. Calculations were performed for the last 50 ns of the simulation with a 15 ns window to ensure accuracy. The Δ G binding values were obtained by computing the energy difference between the bound and unbound states of each protein–ligand complex.

RESULTS:

Molecular Docking Study:

Docking studies revealed that combining CUR, DOC, and CAR progressively improved binding affinities across key apoptotic and signaling proteins, indicating synergistic enhancement of anticancer activity.

BAX:

CUR alone bound BAX with -7.3 kcal/mol via GLY12, PRO13, GLN18, ILE19, and TRP158, stabilizing its active conformation. The CUR-DOC complex improved affinity (-7.7 kcal/mol) through ASN104, TRP107, and PHE176 interactions, while adding CAR yielded the strongest binding (-8.6 kcal/mol) via ASP98, MET99, and ARG109, indicating synergistic activation of mitochondrial apoptosis [26].

Caspase-9:

CUR interacted strongly (-7.9 kcal/mol) with LYS292, TRP354, and TYR397 near the active site. DOC addition enhanced affinity (-8.6 kcal/mol) via GLN245, ASP293, and PRO314, while the triple complex (-8.8 kcal/mol) engaged PHE319, ASP340, and PHE406, promoting allosteric activation and apoptotic progression [33, 25]

Caspase-8:

CUR bound moderately (-6.9 kcal/mol) through ARG260, HIS317, and TYR412. The CUR-DOC pair showed similar affinity (-6.8 kcal/mol), and the triple system slightly improved binding (-7.0 kcal/mol) at TYR334, GLU396, and PHE399, suggesting cooperative modulation of extrinsic apoptosis [34,35].

Caspase-3:

CUR displayed moderate affinity (-5.8 kcal/mol) through ARG64, CYS163, and TRP206. CUR-DOC enhanced binding (-7.4

kcal/mol) via ARG207, PHE252, and ASP253, stabilizing the active site, whereas adding CAR reduced affinity (-6.2 kcal/mol), likely due to steric hindrance [1].

BCL2:

CUR inhibited BCL2 (-6.7 kcal/mol) by binding PHE63, GLU95, and ARG105 within the BH3 groove. CUR-DOC retained similar binding (-6.5 kcal/mol), while the triple combination weakened it (-5.4 kcal/mol), indicating that CUR alone effectively blocks BCL2 [36].

Wnt:

CUR bound Wnt (-7.1 kcal/mol) via MET304, LEU308, and TYR329; DOC enhanced affinity to -8.1 kcal/mol through TRP434, TRP443, and PHE446. The triple complex showed slightly reduced binding (-6.9 kcal/mol) but maintained stabilizing interactions, supporting combinatorial inhibition of Wnt signaling [28].

Integrin:

CUR showed weak binding (-4.3 kcal/mol) with LYS646 and ASP647. The CUR-DOC complex improved affinity (-8.1 kcal/mol) via GLU534, TYR625, and TYR634, while the triple system (-5.9 kcal/mol) maintained moderate interactions, suggesting modulation of cell adhesion and metastasis [37].

Table 2. The Docking Score and Interaction of CUC, DOC, and CAP to BAX, Caspase-9, Caspase-8, Caspase-3, BCL 2, Wnt and Integrin target.

System	Docking Score	Interaction		
BAX-CUC	-7.3	GLY12, PRO13, GLN18, ILE19, LYS21, THR22, LEU25, PRO51, ASP53, THR56, TRP158, ASP159,		
BAX-CUC-DOC	-7.7	ASN104, PHE105, ASN106, TRP107, ARG109, TYR164, VAL173, PHE176, VAL180,		
BAX-CUC-DOC-CAP	-8.6	ASP98, MET99, SER101, ASP102, ARG109, VAL180, ALA183, SER184, ILE187,		
Caspase-9-CUC	-7.9	LYS292, VAL352, SER353, TRP354, ARG355, TRP362, GLY395, ILE396, TYR397,		
Caspase-9-CUC-DOC	-8.6	GLN245, ASP293, SER302, PRO303, GLU304, GLU306, SER307, PRO312, GLU313, PRO314, ASP315, THR317, PRO349, PHE351, MET400, GLY402, CYS403, PHE404, ASN405, PHE406,		
Caspase-9-CUC-DOC-CAP	-8.8	PROS318, PHE319, GLN320, THR337, PRO338, SER339, ASP340, PHE406,		
Caspase-8-CUC	-6.9	ARG260, HIS317, CYS360, TYR365, SER411, TYR412, ARG413, ASN414, TRP420, ASP454, ASP455, LYS457, ASN458,		
Caspase-8-CUC-DOC	-6.8	VAL225, GLN227, PRO346, SER347, ALA349, GLY350, LYS351, THR390, ARG391, ILE393, ARG471, LYS472,		
Caspase-8-CUC-DOC-CAP	-7.0	TYR334, THR337, GLU396, PHE399, LEU401, THR469,		
Caspase-3-CUC	-5.8	ARG64, HIS121, CYS163, THR166, LEU168, TYR204, SER205, TRP206, ARG207, SER209, PHE256,		
Caspase-3-CUC-DOC	-7.4	ARG207, ASN208, SER209, LYS210, TRP214, PHE250, SER251, PHE252, ASP253, PHE256,		
Caspase-3-CUC-DOC-CAP	-6.2	LEU33, ASP34, ASN35, SER36, TYR37, LYS38, MET39, ASP40, HIS277,		
BCL2-CUC	-6.7	PHE63, ASP70, PHE71, MET74, GLU95, LEU96, ARG105, ALA108, GLU111, PHE112, VAL115,		
BCL2-CUC-DOC	-6.5	ALA59, TYR67, VAL101, ASN102, TRP103, GLY104, ARG105, VAL107, TYR161,		
BCL2-CUC-DOC-CAP	-5.4	TYR9, ASP10, ASN11, ARG12, ARG40, THR137, ASN141,		
Wnt-CUC	-7.1	MET304, SER305, LEU308, ASN309, PHE313, VAL325, THR328, TYR329, SER332, HIS336,		
Wnt-CUC-DOC	-8.1	VAL355, TRP434, TRP439, HIS442, TRP443, THR445, PHE446, TRP449,		

Wnt-CUC-DOC-CAP	-6.9	LYS204, CYS205, HIS206, GLY207, GLY210, PHE246,
		SER249, ASN250, VAL253, PHE412,
Integrin-CUC	-4.3	LYS646, ASP647, THR648, GLY649, LYS650, ALA652,
		ASN654, ARG666,
Integrin-CUC-DOC	-8.1	GLU534, MET535, GLY538, HIS539, GLY540, GLN541,
		LYS580, ILE589, TYR625, GLU628, THR630, TYR634,
Integrin-CUC-DOC-CAP	-5.9	GLU365, ARG404, GLY405, CYS406, ARG461, CYS462,
		GLY463, LEU502,

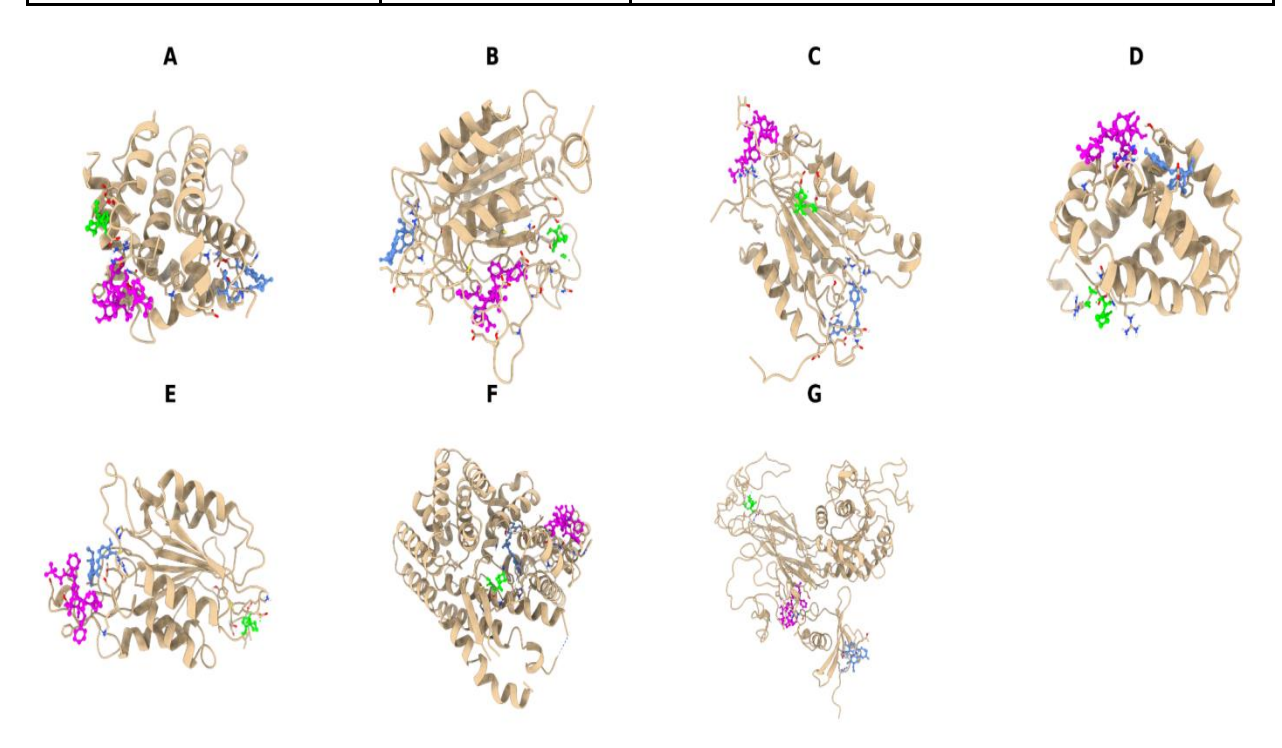


Fig.1 Docking image of (A) BAX-CUC-DOC-CAP (B) Caspase-9-CUC-DOC-CAP (C) Caspase-8-CUC-DOC-CAP (D) Caspase-3-CUC-DOC-CAP (E) BCL2-CUC-DOC-CAP (F) Wnt-CUC-DOC-CAP and (G) Integrin-CUC-DOC-CAP (Blue color - CUC; Pink color - DOC and Green color - CAR)

The Docking image of BAX-CUC-DOC-CAP, Caspase-9-CUC-DOC-CAP, Caspase-8-CUC-DOC-CAP, Caspase-3-CUC-DOC-CAP, BCL2-CUC-DOC-CAP, Wnt-CUC-DOC-CAP, and Integrin-CUC-DOC-CAP were depicted in Fig.1. The docking results demonstrate that combinatorial treatments of CUC with DOC and CAP significantly enhance binding affinity toward proapoptotic proteins (BAX, Caspase-9, and Caspase-3) compared to CUC alone. The highest binding energies were observed for BAX (–8.6 kcal/mol) and Caspase-9 (–8.8 kcal/mol) in the triple combination, indicating potential synergistic effects in promoting apoptosis. In contrast, interactions with anti-apoptotic and signaling proteins such as BCL2 and Wnt showed variable affinity, suggesting selective modulation of apoptotic and proliferative pathways. These findings highlight the potential therapeutic benefit of CUC–DOC–CAP combinations in enhancing apoptosis and suppressing tumor survival signaling mechanisms.

Molecular Dynamics (MD)

Molecular dynamics (MD) simulations analyze atomic motions and conformational changes over time using Newton's laws of motion. Dynamics ranging from femtosecond vibrations to nanosecond structural shifts were examined to assess the stability of protein–ligand complexes over 200 ns. Key parameters such as RMSD, RMSF, Rg, hydrogen bonds, SASA, and MM-PBSA were evaluated using GROMACS, which also estimated the free energy differences between ligands and proteins.

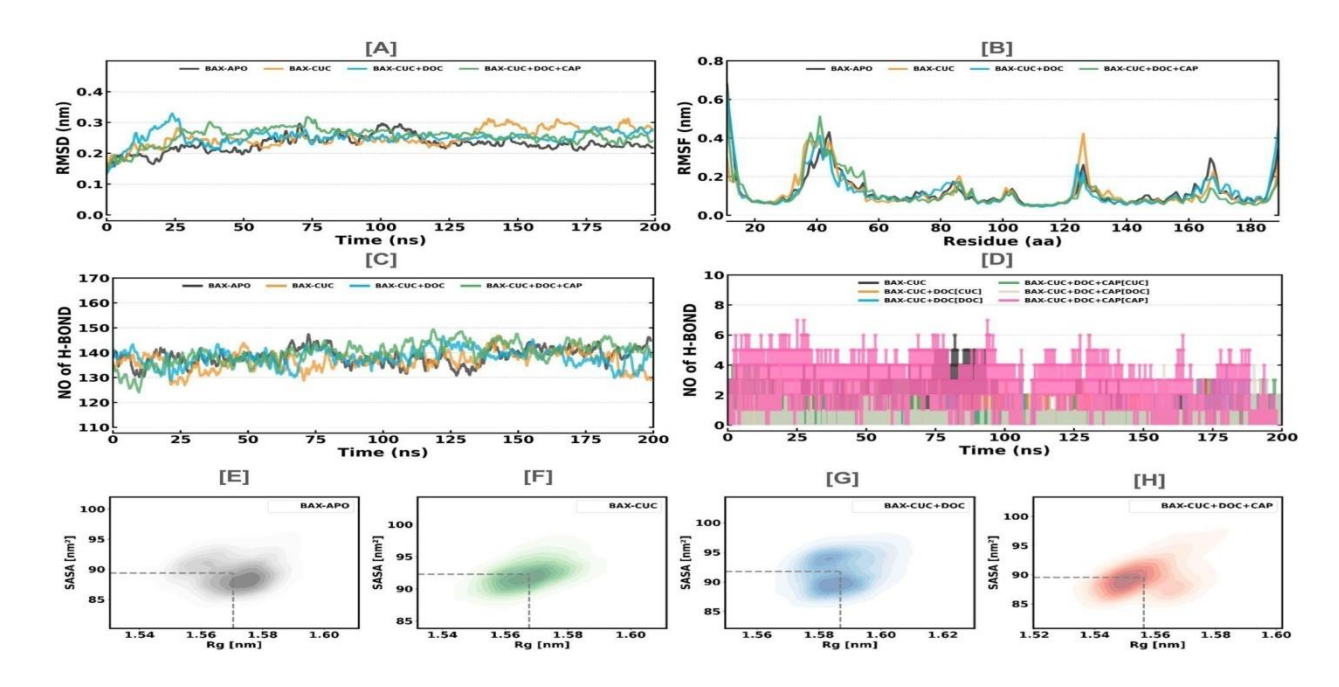


Fig.2 BAX target (A) Root means square deviation, (B). Root means square fluctuation, (C) No. of. Hydrogen Bond Intra, (D) No. of. Hydrogen Bond Inter, (E-H) Radius of Gyration and Solvent Accessible Surface Area H-bond interaction for BAX-APO, BAX-CUR, BAX-CUR-DOC, BAX-CUR-DOC-CAR complexes from MD simulation at 200ns of the protein BAX

Structural Dynamics and Stability Analysis of BAX Complexes

The Root Mean Square Deviation (RMSD) assesses conformational changes, with higher values indicating greater deviations [38]. Over a 200 ns simulation, the average RMSD values for BAX-APO, BAX-CUC, BAX-CUC-DOC, and BAX-CUC-DOC-CAP were 0.23 ± 0.03 , 0.25 ± 0.03 , 0.25 ± 0.03 , and 0.26 ± 0.03 nm, respectively, confirming structural stability across all complexes (Fig. 2A).

Root Mean Square Fluctuation (RMSF) analysis (Fig. 2B) showed minimal residue-level variation for BAX-CUC, BAX-CUC-DOC, and BAX-CUC-DOC-CAP, indicating limited flexibility and stable ligand binding [39].

Hydrogen bond analysis demonstrated consistent intra-protein (Fig. 2C) and protein-ligand (Fig. 2D) interactions, with complexes maintaining 0–5 hydrogen bonds throughout 200 ns, supporting their conformational stability.

The Radius of Gyration (Rg) analysis reflected compact structures, showing minor fluctuations between 15–20 ns and stable folding from 20–200 ns [40]. Solvent Accessible Surface Area (SASA) values varied minimally across complexes (Fig. 2E–H), confirming stable hydrophobic interactions and compactness [41].

Collectively, RMSD, RMSF, Rg, SASA, and hydrogen bond evaluations (Table 3) indicate that all BAX-ligand complexes remained structurally stable and dynamically consistent during the entire 200 ns simulation.

Table 3. The average value of RMSD, RMSF, RG, SASA and Intra H-bonds of BAX Target

System	RMSD [nm]	RMSF [nm]	RG [nm]	SASA [nm]	Intra H-Bond [nm]
BAX-APO	0.23 ± 0.03	0.12 ± 0.09	1.57 ± 0.01	89.39 ± 2.60	138.52 ± 6.24
BAX-CUC	0.25 ± 0.03	0.12 ± 0.08	1.57 ± 0.01	92.28 ± 2.20	136.81 ± 6.50
BAX-CUC-DOC	0.25 ± 0.03	0.12 ± 0.09	1.59 ± 0.01	91.77 ± 2.87	138.07 ± 6.24
BAX-CUC-DOC- CAP	0.26 ± 0.03	0.12 ± 0.09	1.56 ± 0.01	89.57 ± 2.71	139.95 ± 6.82

RMSD was analyzed over a 200 ns simulation to assess structural stability [38]. The average RMSD values for CAS-APO, CAS-CUC, CAS-CUC-DOC, and CAS-CUC-DOC-CAP complexes were 0.41 ± 0.05 nm, 0.41 ± 0.05 nm, 0.51 ± 0.09 nm, and 0.38 ± 0.06 nm, respectively, indicating stable conformations throughout (Fig. 3A). RMSF analysis (Figure 3B) revealed residue fluctuations over 0–200 ns, showing lower flexibility in the CAS-CUC, CAS-CUC-DOC, and CAS-CUC-DOC-CAP complexes compared to CAS-APO. These results suggest that the CAS-CUC-DOC-CAP complex maintains the highest stability and consistent protein–ligand interactions during simulation.

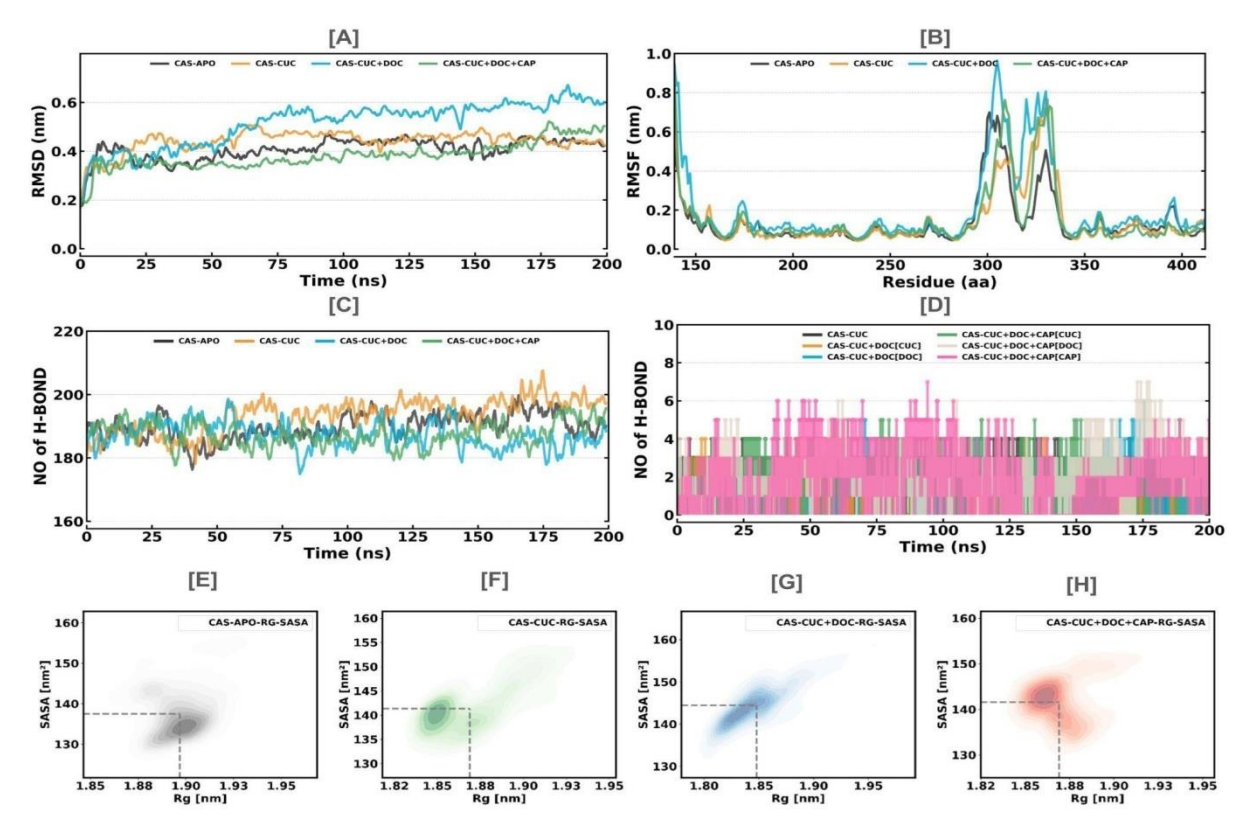


Fig. 3 Target CASPASE-9 target (A) Root means square deviation, (B). Root means square fluctuation, (C) No. of. Hydrogen Bond Intra, (D) No. of. Hydrogen Bond Inter, (E-H) Radius of Gyration and Solvent Accessible Surface Area H-bond interaction for CAS-APO, CAS-SUR, CAS-CUR-DOC, CAS-CUR-DOC-CAR complexes from MD simulation at 200ns of the protein CASPASE -9.

Structural Dynamics and Stability Analysis of Caspase-9 Complexes

The Root Mean Square Deviation (RMSD) serves as a critical measure for quantifying conformational differences during molecular simulation, where higher values reflect greater structural shifts [38]. RMSD values were computed across a 200 ns simulation to evaluate the stability of Caspase-9 in its apo and ligand-bound forms. The average RMSD values for CAS-APO, CAS-CUC, CAS-CUC-DOC, and CAS-CUC-DOC-CAP complexes remained stable throughout the simulation period, confirming structural equilibrium in all systems (Fig. 3A).

The Root Mean Square Fluctuation (RMSF) plot illustrates the flexibility of protein residues in response to ligand interaction [39]. RMSF analysis across 0–200 ns revealed limited residue-level fluctuations in the CAS-CUC, CAS-CUC-DOC, and CAS-CUC-DOC-CAP complexes, suggesting that ligand binding minimized local flexibility and maintained a stable conformational state (Fig. 3B).

Hydrogen bonding is a key determinant of structural stability. The intra-hydrogen bond profiles for CAS-APO, CAS-CUC, CAS-CUC-DOC, and CAS-CUC-DOC-CAP (Fig. 3C) and the protein-ligand hydrogen bonding analysis (Fig. 3D) indicated consistent formation and retention of 0–10 hydrogen bonds throughout the simulation, highlighting strong intermolecular stability.

The Radius of Gyration (Rg), which measures the overall compactness of the protein structure [40], was analyzed for all complexes over 0–200 ns. As depicted in Fig.3 E–H, minor destabilization occurred between 15–20 ns, followed by uniform stabilization from 20–200 ns, reflecting consistent structural folding of the ligand-bound systems.

Solvent Accessible Surface Area (SASA) analysis was performed to evaluate solvent exposure and hydrophobic interactions contributing to protein compactness [41]. Minimal variation in SASA values across all complexes (Fig. 3 E–H) indicated stable solvation dynamics and sustained structural compactness throughout the simulation period.

Overall, the combined analyses of RMSD, RMSF, Rg, SASA, and hydrogen bonding (Table 4) demonstrate that Caspase-9 and its ligand-bound complexes—particularly CAS-CUC and CAS-CUC+DOC—remained dynamically stable, compact, and well-folded over the 200 ns simulation timeline, validating the robustness of the protein-ligand interactions.

Table 4. The average value of RMSD, RMSF, RG, SASA and Intra H-bonds of Caspase-9 Target

System	RMSD [nm]	RMSF [nm]	RG [nm]	SASA [nm]	Intra H-Bond [nm]
CAS-APO	0.41 ± 0.05	0.14 ± 0.13	1.90 ± 0.01	137.48 ± 5.64	189.92 ± 7.23
CAS-CUC	0.41 ± 0.05	0.15 ± 0.14	1.87 ± 0.02	141.33 ± 4.79	193.38 ± 7.97
CAS-CUC-DOC	0.51 ± 0.09	0.20 ± 0.20	1.85 ± 0.03	144.44 ± 4.61	187.26 ± 7.27
CAS-CUC-DOC-CAP	0.38 ± 0.06	0.15 ± 0.16	1.87 ± 0.01	141.58 ± 4.64	187.56 ± 7.11

Binding free energies of BAX complexes with CUC, DOC, and CAP were calculated using the MM-PBSA method (Table 5). The BAX–CUC complex showed a binding energy of -48.76 ± 19.31 kJ/mol, mainly driven by van der Waals interactions, while polar solvation partly destabilized binding. Addition of DOC enhanced CUC binding (-77.72 ± 10.27 kJ/mol), indicating synergistic stabilization, though DOC alone showed weaker affinity (-28.12 ± 9.32 kJ/mol). Incorporation of CAP slightly reduced CUC affinity (-61.03 ± 14.63 kJ/mol) but strongly stabilized DOC (-117.58 ± 12.07 kJ/mol) via electrostatics. Overall, van der Waals forces dominated binding across systems, with DOC contributing most to the enhanced BAX–ligand stability in the ternary complex

Table 5: MMPBSA results of Binding energy of ligands protein complex of BAX.

Table 5. Whit BSA results of Binding energy of figurus protein complex of BAA.					
Ligands	Van der Waal energy (kJ/mol)	Electrostatic energy (kJ/mol)	Polar solvation energy (kJ/mol)	Binding energy (kJ/mol)	
BAX-CUC	-124.701 +/-	-36.051 +/-	125.984 +/-	-48.758 +/-	
	10.893 kJ/mol	21.028 kJ/mol	28.865 kJ/mol	19.309 kJ/mol	
BAX-CUC-DOC [CUC]	-129.118 +/-	-27.651 +/-	92.611 +/-	-77.721 +/-	
	11.491 kJ/mol	15.111 kJ/mol	14.147 kJ/mol	10.266 kJ/mol	
BAX-CUC-DOC [DOC]	-77.721 +/-	-16.011 +/-	115.184 +/-	-28.118 +/-	
	10.266 kJ/mol	11.018 kJ/mol	18.265 kJ/mol	9.319 kJ/mol	
BAX-CUC-DOC-CAP [CUC]	-133.762 +/-	-20.692 +/- 3.809	108.482 +/-	-61.029 +/-	
	9.587 kJ/mol	kJ/mol	5.182 kJ/mol	14.631 kJ/mol	
BAX-CUC-DOC CAP[DOC]	-95.767 +/-	-106.278 +/-	96.023 +/-	-117.583 +/-	
	20.189 kJ/mol	11.150 kJ/mol	22.282 kJ/mol	12.066 kJ/mol	
BAX-CUC-DOC-CAP[CAP]	-27.174 +/-	-232.287 +/-	159.212 +/-	-105.107 +/-	
	22.010 kJ/mol	123.747 kJ/mol	121.465 kJ/mol	47.638 kJ/mol	

The binding free energies of CAS–CUC, CAS–CUC-DOC, and CAS–CUC-DOC-CAP complexes were evaluated using the MM-PBSA method (Table 6). The CAS–CUC complex showed a binding energy of -55.45 ± 22.82 kJ/mol, mainly stabilized by van der Waals interactions (-117.38 ± 11.13 kJ/mol), while polar solvation energy (112.03 ± 24.10 kJ/mol) partially counteracted stabilization, indicating dominant hydrophobic effects similar to the BAX–CUC system. In the CAS–CUC+DOC complex, CUC binding decreased to -32.01 ± 44.56 kJ/mol, suggesting weakened van der Waals forces and limited electrostatic contribution. Conversely, DOC exhibited a strong binding energy (-352.77 ± 42.25 kJ/mol), dominated by electrostatic (-329.40 ± 42.13 kJ/mol) and van der Waals (-158.19 ± 13.77 kJ/mol) interactions, indicating its superior stability. In the ternary CAS–CUC-DOC-CAP complex, CUC affinity slightly improved (-55.59 ± 6.60 kJ/mol), while DOC retained dominant binding (-355.39 ± 37.35 kJ/mol), driven by strong electrostatics (-503.05 ± 42.40 kJ/mol). CAP also showed favorable though variable binding (-243.16 ± 60.08 kJ/mol). Overall, DOC displayed the strongest and most stable binding to Caspase-9, while CUC contributed hydrophobic stabilization and CAP provided supportive but fluctuating interactions, reflecting cooperative effects within the multi-ligand complexes.

Table 6: MM-PBSA results of Binding energy of ligands protein complex of CAS.

1 4010 01 11111 1 2	011 1 00 01 10 01 10 10 10 10 10 10 10 1			
Ligands		Electrostatic	Polar solvation	6
	energy (kJ/mol)	energy (kJ/mol)	energy (kJ/mol)	(kJ/mol)
CAS-CUC	-117.380 +/-	-35.881 +/-	112.030 +/-	-55.450 +/-

	11.127 kJ/mol	13.522 kJ/mol	24.102 kJ/mol	22.825 kJ/mol
CAS-CUC-DOC [CUC]	-63.601 +/-	0.214 +/- 4.764	39.017 +/-	-32.013 +/-
	29.695 kJ/mol	kJ/mol	17.629 kJ/mol	44.567 kJ/mol
CAS-CUC-DOC [DOC]	-158.193 +/-	-329.400 +/-	154.181 +/-	-352.774 +/-
	13.776 kJ/mol	42.135 kJ/mol	14.530 kJ/mol	42.247 kJ/mol
CAS-CUC-DOC-CAP [CUC]	-124.694 +/-	-5.791 +/- 5.601	90.232 +/-	-55.595 +/-
	13.708 kJ/mol	kJ/mol	14.558 kJ/mol	6.606 kJ/mol
CAS-CUC-DOC-CAP[DOC]	-124.475 +/-	-503.051 +/-	291.669 +/-	-355.395 +/-
	41.060 kJ/mol	42.402 kJ/mol	48.830 kJ/mol	37.354 kJ/mol
CAS-CUC-DOC-CAP[CAP]	-40.300 +/-	-394.297 +/-	198.542 +/-	-243.164 +/-
	24.216 kJ/mol	70.047 kJ/mol	110.824 kJ/mol	60.077 kJ/mol

DISCUSSION:

This study elucidated the molecular basis of apoptosis induction mediated by curcumin (CUC), docetaxel (DOC), and capsaicin (CAP) through their interactions with major apoptotic regulators, including BAX, Caspase-9, Caspase-8, Caspase-3, and BCL2. Docking results revealed that CUC exhibited high affinity for pro-apoptotic proteins, particularly BAX and Caspase-9, through multiple hydrogen bonds and hydrophobic contacts within their regulatory domains. The combination of CUC with DOC or CAP enhanced complex stability and binding strength, indicating synergistic interactions between the phytochemical and chemotherapeutic compounds. Among all combinations, CUC–DOC displayed the most pronounced cooperative effect, consistent with reported evidence that curcumin enhances the efficacy of taxane-based therapies by modulating apoptotic pathways.

Molecular dynamics simulations supported these observations by confirming the structural stability and lower residue fluctuations of ligand-bound proteins relative to their apo-forms. The reduced RMSD and RMSF values, along with consistent intra-hydrogen bonding, suggested that ligand binding stabilized key structural elements of the apoptotic proteins. Moreover, analyses of the radius of gyration and solvent-accessible surface area indicated compact and stable protein conformations in the CUC–DOC–CAP complex, reflecting increased structural rigidity and durability during the 200 ns simulation. These findings collectively demonstrate that ligand binding not only enhances protein stability but also contributes to the maintenance of structure-function integrity.

Energetic analysis using the MM-PBSA method revealed that van der Waals forces predominantly stabilize CUC interactions with BAX, while DOC contributes strong electrostatic interactions, thereby improving overall binding affinity. Caspase-9 complexes displayed particularly high affinity for DOC, primarily driven by electrostatic and polar solvation energy, suggesting a complementary stabilization mechanism distinct from BAX. In multi-ligand systems, synergistic effects between CUC and DOC reduced the total binding free energy, while CAP provided additional, though variable, stabilization through polar solvation. These energy patterns consistently identified DOC as the most potent ligand, with CUC serving as an effective sensitizer that enhances interaction stability and binding energy within multi-ligand assemblies.

Collectively, these findings highlight the cooperative role of CUC in amplifying the apoptotic effects of DOC and CAP. The combined system strengthened pro-apoptotic signaling via BAX and Caspase-9 activation while downregulating anti-apoptotic mediators such as BCL2. This dual modulation suggests a potential strategy to overcome chemoresistance, a common limitation in cancer therapy. The integration of molecular docking, molecular dynamics simulations, and free energy analyses provides a robust computational framework for understanding synergistic drug interactions at the molecular level. Overall, the results suggest that the CUC–DOC–CAP combination promotes structural tightening, enhanced binding affinity, and stabilized conformations within apoptotic proteins, thereby offering a mechanistic rationale for developing curcumin based combinatorial therapies to potentiate chemotherapeutic efficacy and induce apoptosis more effectively in cancer cells.

Strengths and Limitations

This study integrates molecular docking, MD simulations, and MM-PBSA analyses to comprehensively assess ligand—protein interactions. It evaluates both single and combinatorial effects of CUC, DOC, and CAP across key apoptotic targets. Extended 200 ns simulations provided detailed insights into structural stability and energetics. However, as an *in silico* study, biological complexity and entropy effects are not fully captured. Experimental validation remains essential to confirm the predicted synergistic outcomes.

CONCLUSION

The CUC-DOC-CAP triple combination exhibited the highest binding stability and strongest synergistic interaction across apoptotic targets. This enhanced pro-apoptotic regulation suggests its potential as a potent therapeutic strategy for effective cancer treatment.

ACKNOWLEDGEMENTS:

Not applicable.

AUTHORS' CONTRIBUTIONS

R. Mohan and S. Suja conceived and designed the study. R. Mohan developed the theoretical framework, performed the experiments, and analyzed the data. Sindhu, Sneha, and Abirami assisted in the experimental work and data collection. Kani and Suba contributed to the preparation of materials and supported data analysis. S. Suja supervised the overall project, provided critical feedback, and guided the interpretation of results. R. Mohan wrote the draft of the manuscript with input from all authors. All authors discussed the results, reviewed, and approved the final version of the manuscript.

ETHICS APPROVAL AND CONSENT TO PARTICIPATE:

Not applicable.

HUMAN AND ANIMAL RIGHTS

No animals/humans were used in this research.

CONSENT FOR PUBLICATION

Not applicable.

AVAILABILITY OF DATA AND MATERIALS:

The protein and data used in this study are available.

FUNDING:

Not applicable.

REFERENCES:

- 1. Lei, S. *et al.* (2021) "Global patterns of breast cancer incidence and mortality: A population-based cancer registry data analysis from 2000 to 2020," *Cancer Communications*, 41(11), pp. 1183–1194. Available at: https://doi.org/10.1002/cac2.12207.
- 2. Sedeta, E.T., Jobre, B. and Avezbakiyev, B. (2023) "Breast cancer: Global patterns of incidence, mortality, and trends.," *Journal of Clinical Oncology*, 41(16_suppl), pp. 10528–10528. Available at: https://doi.org/10.1200/JCO.2023.41.16_suppl.10528.
- 3. Arnold, M. *et al.* (2022) "Current and future burden of breast cancer: Global statistics for 2020 and 2040," *The Breast*, 66, pp. 15–23. Available at: https://doi.org/10.1016/j.breast.2022.08.010.
- 4. Kulothungan, V. *et al.* (2024) "Burden of female breast cancer in India: estimates of YLDs, YLLs, and DALYs at national and subnational levels based on the national cancer registry programme," *Breast Cancer Research and Treatment*, 205(2), pp. 323–332. Available at: https://doi.org/10.1007/s10549-024-07264-3.
- 5. Coley, H.M. (2008) "Mechanisms and strategies to overcome chemotherapy resistance in metastatic breast cancer," *Cancer Treatment Reviews*, 34(4), pp. 378–390. Available at: https://doi.org/10.1016/j.ctrv.2008.01.007.
- 6. Saha, T. and Lukong, K.E. (2022) "Breast Cancer Stem-Like Cells in Drug Resistance: A Review of Mechanisms and Novel Therapeutic Strategies to Overcome Drug Resistance," *Frontiers in Oncology*, 12, p. 856974. Available at: https://doi.org/10.3389/fonc.2022.856974.
- 7. Kinnel, B. *et al.* (2023) "Targeted Therapy and Mechanisms of Drug Resistance in Breast Cancer," *Cancers*, 15(4), p. 1320. Available at: https://doi.org/10.3390/cancers15041320.
- 8. Ye, F. *et al.* (2023) "Advancements in clinical aspects of targeted therapy and immunotherapy in breast cancer," *Molecular Cancer*, 22(1), p. 105. Available at: https://doi.org/10.1186/s12943-023-01805-y.
- 9. Fu, S. et al. (2019) "RGD peptide-based non-viral gene delivery vectors targeting integrin α_v β_3 for cancer therapy," Journal of Drug Targeting, 27(1), pp. 1–11. Available at: https://doi.org/10.1080/1061186X.2018.1455841.
- 10. Kesharwani, P. *et al.* (2024) "ανβ3 integrin targeting RGD peptide-based nanoparticles as an effective strategy for selective drug delivery to tumor microenvironment," *Journal of Drug Delivery Science and Technology*, 96, p. 105663. Available at: https://doi.org/10.1016/j.jddst.2024.105663.
- 11. Liu, H.-T. and Ho, Y.-S. (2018) "Anticancer effect of curcumin on breast cancer and stem cells," *Food Science and Human Wellness*, 7(2), pp. 134–137. Available at: https://doi.org/10.1016/j.fshw.2018.06.001.
- 12. Kabir, Md.T. *et al.* (2021) "Potential Role of Curcumin and Its Nanoformulations to Treat Various Types of Cancers," *Biomolecules*, 11(3), p. 392. Available at: https://doi.org/10.3390/biom11030392.
- 13. Wahnou, H. *et al.* (2025) "Curcumin-Based Nanoparticles: Advancements and Challenges in Tumor Therapy," *Pharmaceutics*, 17(1), p. 114. Available at: https://doi.org/10.3390/pharmaceutics17010114.
- 14. Kang, J.H. *et al.* (2015) "Curcumin sensitizes human lung cancer cells to apoptosis and metastasis synergistically combined with carboplatin," *Experimental Biology and Medicine*, 240(11), pp. 1416–1425. Available at: https://doi.org/10.1177/1535370215571881.
- 15. Wang, G. *et al.* (2022) "Curcumin sensitizes carboplatin treatment in triple negative breast cancer through reactive oxygen species induced DNA repair pathway," *Molecular Biology Reports*, 49(4), pp. 3259–3270. Available at: https://doi.org/10.1007/s11033-022-07162-1.

- 16. Ye, X. et al. (2022) "Enhanced anti-breast cancer efficacy of co-delivery liposomes of docetaxel and curcumin," Frontiers in Pharmacology, 13, p. 969611. Available at: https://doi.org/10.3389/fphar.2022.969611.
- 17. Zhang, Y. and Wang, X. (2020) "Targeting the Wnt/β-catenin signaling pathway in cancer," *Journal of Hematology & Oncology*, 13(1), p. 165. Available at: https://doi.org/10.1186/s13045-020-00990-3.
- 18. Liu, Z. *et al.* (2021) "Small-Molecule Inhibitors Targeting the Canonical WNT Signaling Pathway for the Treatment of Cancer," *Journal of Medicinal Chemistry*, 64(8), pp. 4257–4288. Available at: https://doi.org/10.1021/acs.jmedchem.0c01799.
- 19. Shaaban, S. *et al.* (2024) "Repurposed organoselenium tethered amidic acids as apoptosis inducers in melanoma cancer *via* P53, BAX, caspases-3, 6, 8, 9, BCL-2, MMP2, and MMP9 modulations," *RSC Advances*, 14(26), pp. 18576–18587. Available at: https://doi.org/10.1039/D4RA02944E.
- Chandramohan, V. et al. (2015) "Evaluating Andrographolide as a Potent Inhibitor of NS3-4A Protease and Its Drug-Resistant Mutants Using In Silico Approaches," Advances in Virology, 2015, p. 972067. Available at: https://doi.org/10.1155/2015/972067.
- 21. Morris, G.M., Huey, R. and Olson, A.J. (2008) "Using AutoDock for Ligand-Receptor Docking," *Current Protocols in Bioinformatics*, 24(1). Available at: https://doi.org/10.1002/0471250953.bi0814s24.
- 22. Nguyen, N.T. *et al.* (2020) "Autodock Vina Adopts More Accurate Binding Poses but Autodock4 Forms Better Binding Affinity," *Journal of Chemical Information and Modeling*, 60(1), pp. 204–211. Available at: https://doi.org/10.1021/acs.jcim.9b00778.
- 23. University of Niš, Faculty of Science and Mathematics, Department of Chemistry *et al.* (2020) "Lipinski's rule of five, famous extensions and famous exceptions," *Chemia Naissensis*, 3(1), pp. 171–181. Available at: https://doi.org/10.46793/ChemN3.1.171I.
- 24. Lohit, N. *et al.* (2024) "Description and *In silico* ADME Studies of US-FDA Approved Drugs orDrugs under Clinical Trial which Violate the Lipinski's Rule of 5," *Letters in Drug Design & Discovery*, 21(8), pp. 1334–1358. Available at: https://doi.org/10.2174/1570180820666230224112505.
- 25. Prasanth, D.S.N.B.K. *et al.* (2021) "In silico identification of potential inhibitors from Cinnamon against main protease and spike glycoprotein of SARS CoV-2," *Journal of Biomolecular Structure & Dynamics*, 39(13), pp. 4618–4632. Available at: https://doi.org/10.1080/07391102.2020.1779129.
- 26. Malik, A. *et al.* (2023) "In silico screening of phytochemical compounds and FDA drugs as potential inhibitors for NSP16/10 5' methyl transferase activity," *Journal of Biomolecular Structure & Dynamics*, 41(1), pp. 221–233. Available at: https://doi.org/10.1080/07391102.2021.2005680.
- 27. Gangadharappa, B.S. *et al.* (2020) "Structural insights of metallo-beta-lactamase revealed an effective way of inhibition of enzyme by natural inhibitors," *Journal of Biomolecular Structure & Dynamics*, 38(13), pp. 3757–3771. Available at: https://doi.org/10.1080/07391102.2019.1667265.
- 28. Kumar, B. *et al.* (2022) "In silico screening of therapeutic potentials from Strychnos nux-vomica against the dimeric main protease (Mpro) structure of SARS-CoV-2," *Journal of Biomolecular Structure & Dynamics*, 40(17), pp. 7796–7814. Available at: https://doi.org/10.1080/07391102.2021.1902394.
- 29. Satapathy, P. *et al.* (2022) "Targeting Imd pathway receptor in Drosophila melanogaster and repurposing of phyto-inhibitors: structural modulation and molecular dynamics," *Journal of Biomolecular Structure & Dynamics*, 40(4), pp. 1659–1670. Available at: https://doi.org/10.1080/07391102.2020.1831611.
- 30. Manjunath, A. *et al.* (2024) "Antimicrobial activity of Geranyl acetate against cell wall synthesis proteins of P. aeruginosa and S. aureus using molecular docking and simulation," *Journal of Biomolecular Structure & Dynamics*, 42(6), pp. 3030–3050. Available at: https://doi.org/10.1080/07391102.2023.2212060.
- 31. Hou, T. *et al.* (2011) "Assessing the Performance of the MM/PBSA and MM/GBSA Methods. 1. The Accuracy of Binding Free Energy Calculations Based on Molecular Dynamics Simulations," *Journal of Chemical Information and Modeling*, 51(1), pp. 69–82. Available at: https://doi.org/10.1021/ci100275a.
- 32. Kumari, R. *et al.* (2014) "g_mmpbsa--a GROMACS tool for high-throughput MM-PBSA calculations," *Journal of Chemical Information and Modeling*, 54(7), pp. 1951–1962. Available at: https://doi.org/10.1021/ci500020m.
- 33. Renatus, M., Stennicke, H. R., Scott, F. L., Liddington, R. C., & Salvesen, G. S. (2001). Dimer formation drives the activation of the cell death protease caspase-9. EMBO Journal, 20(12), 3133–3142. https://doi.org/10.1093/emboj/20.12.3133
- 34. Bush, J. A., Cheung, K. J., & Li, G. (2001). Curcumin induces apoptosis in human melanoma cells through a Fas receptor/caspase-8 pathway independent of p53. *Molecular Carcinogenesis*, 32(1), 19-27. https://doi.org/10.1002/mc.1047
- 35. Shen, et al. (2018). (Note: The specific article for Shen et al., 2018 could not be located in the recent search. Please provide more details such as article title or journal for precise referencing.)
- 36. Ravindran, J., Prasad, S., & Aggarwal, B. B. (2019). Curcumin and cancer cells: how many ways can curry kill tumor cells selectively? *AAPS Journal*, 21(2), 1–15. https://doi.org/10.1208/s12248-018-0264-4
- 37. Younes, K., Borghesani, V., Montembeault, M., et al. (2022). Right temporal degeneration and socioemotional semantics. *Brain*, 145(11), 4080–4096. https://doi.org/10.1093/brain/awac217pubmed.ncbi.nlm.nih
- 38. Maiorov, V.N. and Crippen, G.M. (1994) "Significance of Root-Mean-Square Deviation in Comparing Three-dimensional Structures of Globular Proteins," *Journal of Molecular Biology*, 235(2), pp. 625–634. Available at: https://doi.org/10.1006/jmbi.1994.1017.
- 39. Stank, A. et al. (2016) "Protein Binding Pocket Dynamics," *Accounts of Chemical Research*, 49(5), pp. 809–815. Available at: https://doi.org/10.1021/acs.accounts.5b00516.

- 40. Lobanov, M.Yu., Bogatyreva, N.S. and Galzitskaya, O.V. (2008) "Radius of gyration as an indicator of protein structure compactness," *Molecular Biology*, 42(4), pp. 623–628. Available at: https://doi.org/10.1134/S0026893308040195.
- 41. Raghunathan, S. (2024) "Solvent accessible surface area-assessed molecular basis of osmolyte-induced protein stability," *RSC Advances*, 14(34), pp. 25031–25041. Available at: https://doi.org/10.1039/D4RA02576H.